4

Non linear Systems: Introduction

4.1 Introduction

Linear systems are important as models, but the phenomena in nature and technology that cannot be modeled by linear systems are abundant. The reasons are either that the linear model is often only an approximation, which may neglect important factor affecting the dynamics of the system, such as saturation effects and quantization effects, or more importantly, that the system is intrinsically nonlinear because the forces and influences on the system are nonlinear, such as gravitational and electrostatic forces in Physics, or epidemic processes and neuronal activity in Biology.

We return therefore to general nonlinear systems described by (1.3) and (1.4) in continuous-time, and by (1.7) and (1.8) in discrete-time. In the sequel, we will study most of the time autonomous systems, i.e. systems without an input signal. They already have a very rich set of possible dynamics. We also do usually not specify an output signal and limit our attention to the time evolution of the states. Therefore, we consider systems described by

$$\frac{dx}{dt}(t) = F(x(t)) \tag{4.1}$$

in continuous-time, and by

$$x(t+1) = F(x(t)) \tag{4.2}$$

in discrete-time, where $x \in \mathbb{R}^n$. n is called the order of the system.

We are interested in particular in the asymptotic behavior of the solutions of (4.1) and (4.2), i.e. in the behavior as $t \to +\infty$. As we saw in Chapter 2, in the case of linear autonomous systems, where $F(x) = Ax$, with A is an $n \times n$ matrix, the possible asymptotic behaviors are:

1. Convergence to an asymptotically stable equilibrium point (which is unique if A is invertible (For hyperbolic systems, the origin is the only possible equilibrium)),
2. Periodic oscillation, depending on the initial condition,
3. Divergence to infinity.

The different behaviors can be distinguished simply by looking at the eigenvalues of the state matrix A. The situation for nonlinear systems is much more complex. We introduce the different nonlinear phenomena by looking at some example systems.

4.2 Examples

4.2.1 Example 1: Iterations of the logistic map

The simplest discrete-time dynamical system is given by the iterations of an interval on the real line. Given $F : I \to I$ with $I \subset \mathbb{R}$, the corresponding first-order dynamical system is defined by (4.2), with $n = 1$. Each initial state $x(0)$ generates a trajectory $\{(t, x(t)) \mid t \in \mathbb{N}\}$, which we also write as $x(t)$ using a shorter notation, when there is no ambiguity. We are interested in the asymptotic properties of $x(t)$ as $t \to +\infty$. This system is autonomous, i.e. it has no input signal, and no output signal is specified. As a particular example, we take $F(x) = 1 - \lambda x^2$, which leaves the interval $I = [-1, 1]$ invariant, as long as $0 < \lambda \leq 2$. In fact, we consider f restricted to $[-1, 1]$ and take $\Omega = [-1, 1]$. It is usually called the logistic map. Actually, the logistic map is usually the map $F(x) = ax(1 - x)$, where $0 < a \leq 4$ is a parameter. The two maps can be transformed into each other, up to a constant, by mapping the interval $[-1, 1]$ to the interval $[0, 1]$, using the transformation $z = (x + 1)/2$. In other words, we analyze the asymptotic behavior of the solutions of

$$x(t + 1) = 1 - \lambda x^2(t), \tag{4.3}$$

which depends on the value of λ. Figure 4.1 shows different trajectories $x(t)$ of the logistic map system. For $\lambda = 0.6$, all solutions converge to the fixed point of F. This means that the ω-limit set of any solution is the fixed point, and the fixed point is the unique attractor of the system.

For $\lambda = 0.9$, the typical solutions asymptotically oscillate between two values, i.e. they converge towards a cycle (periodic solution) of period 2. Their ω-limit sets are composed of the two points of the period 2 orbit. This is also the unique attractor of the system. There are also some non typical solutions, e.g. the constant solution at the fixed point. Its ω-limit set is obviously the fixed point, but this is not an attractor.

For $\lambda = 1.3$, the typical solutions converge towards a cycle of period 4. Their ω-limit set is composed of the 4 points of the 4-periodic orbit, and this is also the attractor of the system.

For $\lambda = 1.4009$, the typical solutions converge towards a cycle of period 64. Their ω-limit set is composed of the 64 points of the 64-periodic orbit, and this is also the attractor of the system.

Finally, for $\lambda = 1.6$, the typical solutions have an irregular asymptotic, chaotic behavior. Their ω-limit sets cover a whole interval, and this is also the attractor of the system. There are also many non-typical solutions that are periodic. Their ω-limit sets sets are the corresponding periodic orbits. They are usually part of the attractor, but by far are not the whole attractor.

4.2.2 Example 2: Van der Pol Oscillator

A relatively simple continuous time system is the Van der Pol oscillator. It is usually described by the second order differential equation

$$\frac{d^2x}{dt^2}(t) + \lambda \left(x^2(t) - 1\right) \frac{dx}{dt}(t) + x(t) = 0, \tag{4.4}$$

which can be recast as a second-order system of two state equations

$$\dot{x}_1 = x_2 \tag{4.5}$$

$$\dot{x}_2 = -x_1 - \lambda \left(x_1^2 - 1\right) x_2. \tag{4.6}$$

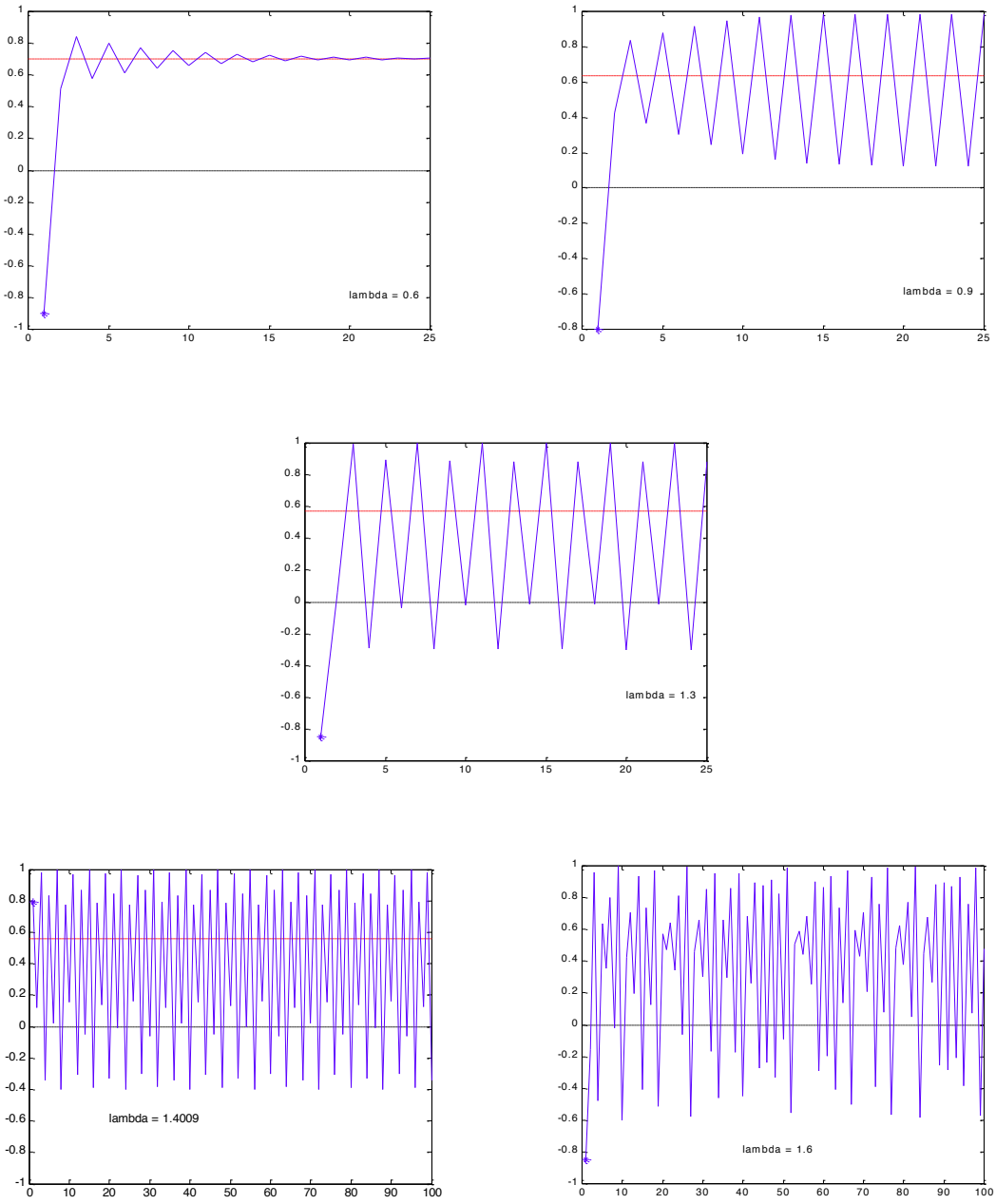

Figure 4.1: Trajectory $x(t)$ for $x(0) = -0.9$ and $\lambda = 0.6$ (top left), $x(0) = -0.8$ and $\lambda = 0.9$ (top right), $x(0) = -0.85$ and $\lambda = 1.3$ (center), $x(0) = -0.791$ and $\lambda = 1.4009$ (bottom left) and $x(0) = -0.85$ and $\lambda = 1.6$(bottom right).

The system has an equilibrium point in $(0, 0)$, which may or may not be stable, depending on the sign of λ. When it is stable, the solutions starting not too far from it converge to it, whereas the solutions starting far from it diverge to infinity. The converging solutions have the equilibrium point as ω-limit set, whereas the diverging solutions have an empty ω-limit set. As an exception, there is also a periodic solution. Its orbit is also its limit set. However, the attractor of the system is just the equilibrium point. Some orbits of the system with a stable equilibrium at the origin are shown on the left part of Figure 4.2.

When it is unstable, the trajectories converge to a limit cycle (periodic solution). Their ω-limit set is the orbit of the limit cycle. This is also the attractor of the system. The constant solution at the equilibrium point is an exception. Its ω-limit set obviously is just the equilibrium point. However it is not part of the attractor. Some orbits of the system with an unstable equilibrium at the origin are shown on the right part of Figure 4.2.

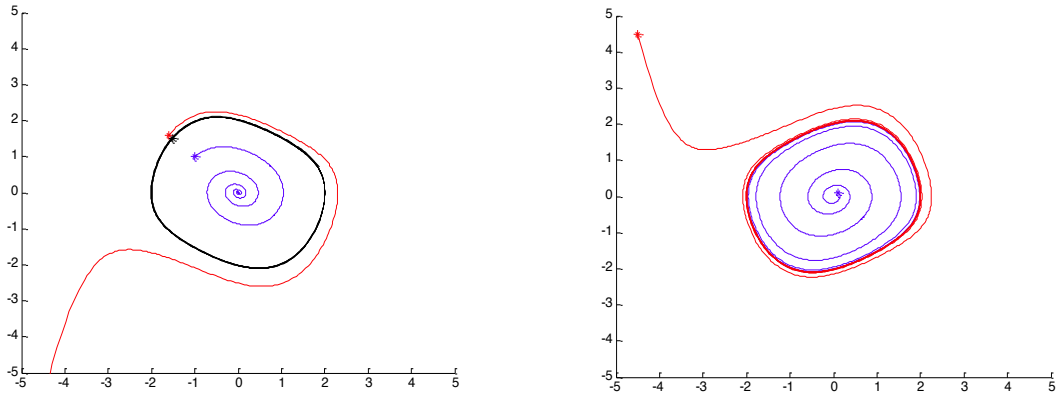

Figure 4.2: Some orbits of the Van der Pol oscillator, with $\lambda = -0.3$ (left): one converging to the equilibrium point, one periodic and the third one diverging to infinity, and with $\lambda = 0.3$ (right): both converging to a limit cycle.

4.2.3 Example 3: Two Coupled Van der Pol Oscillators

We consider the system of two coupled Van der Pol oscillators. The first oscillator is, apart from the coupling term, identical to (4.5) and (4.6). The second has a different basic oscillation frequency ω. The state equations of the two coupled oscillators read

$$\begin{aligned} \dot{x}_1 &= x_2 && (4.7)\\ \dot{x}_2 &= -x_1 - \lambda\left(x_1^2 - 1\right) x_2 + \varepsilon(x_4 - x_2) && (4.8)\\ \dot{x}_3 &= x_4 && (4.9)\\ \dot{x}_4 &= -\omega^2 x_3 - \lambda\left(x_3^2 - 1\right) x_4 + \varepsilon(x_2 - x_4). && (4.10) \end{aligned}$$

If the coupling constant ε is 0 and if $\lambda > 0$, the two oscillators move independently and approach their asymptotic periodic solution as in Section 4.2.2. If $\omega \neq 1$, the two periodic solutions have a different frequency. If the ratio of the two frequencies is irrational, the combined system has a torus as an attractor, namely the cartesian product of the two periodic orbits.

Let us explain that in more detail:

The two periodic trajectories can be parametrized by an "angle variable" (think of the change of polar coordinates that we did in (2.44) in the case of a linear system with complex eigenvalues of the state

matrix). Let

$$x_{(1)} = \begin{bmatrix} x_1 \\ x_2 \end{bmatrix} \quad x_{(2)} = \begin{bmatrix} x_3 \\ x_4 \end{bmatrix},$$

we can write

$$\begin{aligned} x_{(1)} &= f_1(\varphi_1) \\ x_{(2)} &= f_2(\varphi_2) \end{aligned}$$

where $f_i : [0, 2\pi] \to \mathbb{R}^2$, with $i \in \{1, 2\}$, are two continuous, injective functions with $f_i(2\pi) = f_i(0)$. The parametrization can be chosen in such a way that the angles φ_1, φ_2 increase at a constant rate as functions of time, i.e. $\varphi_i = 2\pi(t/T_i)$ with $i \in \{1, 2\}$ where T_1, T_2 are two periods (as for example in (2.46) for the linear system in polar coordinates, with $2\pi/\beta$ as the period):

$$\begin{aligned} x_{(1)}(t) &= f_1(2\pi t/T_1) \\ x_{(2)}(t) &= f_2(2\pi t/T_2). \end{aligned}$$

In general, a closed curve in $\mathbb{R}^n$ is described by a continuous, injective function $f : [0, 2\pi] \to \mathbb{R}^n$ with $f(2\pi) = f(0)$. Similarly, a (2-dimensional) torus in $\mathbb{R}^n$ is described by a continuous, injective function $F : [0, 2\pi]^2 \to \mathbb{R}^n$ with $F(2\pi, \varphi_2) = F(0, \varphi_2)$ and $F(\varphi_1, 2\pi) = F(\varphi_1, 0)$, as shown in Figure 4.3.

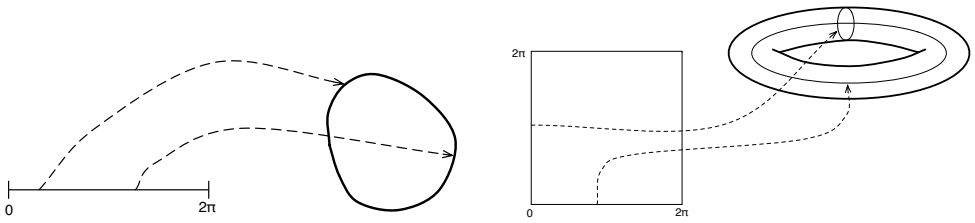

Figure 4.3: Parametrization of a close curve (left) and of a torus (right).

From the two closed curves in $\mathbb{R}^2$, we can now construct a torus in $\mathbb{R}^4$ by taking the Cartesian product:

$$\begin{bmatrix} x_1 \\ x_2 \\ x_3 \\ x_4 \end{bmatrix} = \begin{bmatrix} x_{(1)} \\ x_{(2)} \end{bmatrix} = F\begin{pmatrix} \varphi_1 \\ \varphi_2 \end{pmatrix} = \begin{bmatrix} f_1(\varphi_1) \\ f_2(\varphi_2) \end{bmatrix}.$$

If we now consider the two corresponding periodic solutions, the combined solution of (4.7)-(4.10) becomes

$$\begin{bmatrix} x_1(t) \\ x_2(t) \\ x_3(t) \\ x_4(t) \end{bmatrix} = F\begin{pmatrix} 2\pi t/T_1 \\ 2\pi t/T_2 \end{pmatrix} = \begin{bmatrix} f_1(2\pi t/T_1) \\ f_2(2\pi t/T_2) \end{bmatrix}.$$

If T_1/T_2 is a rational number, the solution on the torus is a closed curve and its ω-limit set obviously is this closed curve. However, since any point on the torus can be taken as initial condition leading to a similar closed curve, the closed curves fill out the whole torus, which is the attractor of the system.

If T_1/T_2 is an irrational number, a single solution gets arbitrarily close to any point on the torus. Hence, its ω-limit set is the whole torus and the attractor is also the torus.

A solution of the juxtaposed van der Pol oscillators starting from a state close to the origin is represented in Figure 4.4. On the left part, x_2 is plotted against x_1: This is nothing else than the orbit

of the first oscillator. On the right part, x_3 is plotted against x_1. This amounts to the combination of a horizontal and a vertical oscillation at different frequencies. If the ratio T_1/T_2 is irrational, this 2-dimensional projection of the 4-dimensional orbit fills out a rectangle, or rather, gets arbitrarily close to any point in the rectangle. Of course, a solution of finite length as in this figure cannot fill out a region. However, it is rather well distributed over the rectangle.

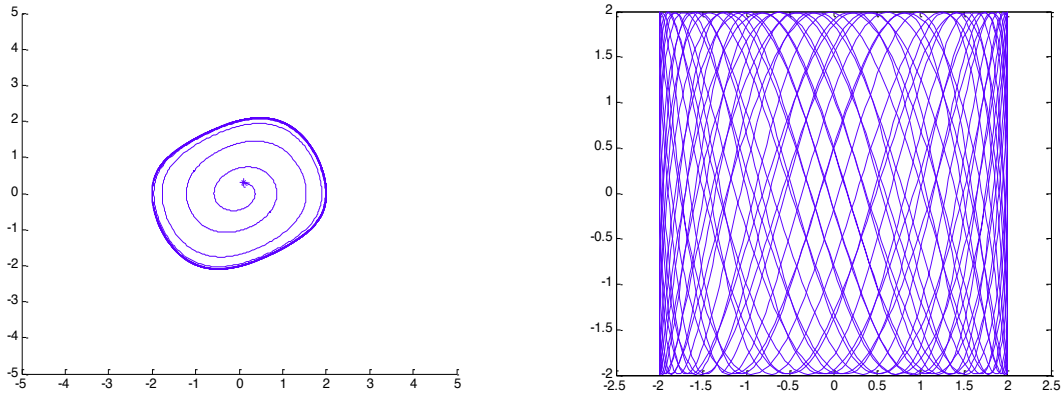

Figure 4.4: Orbits of two juxtaposed (uncoupled: $\varepsilon = 0$) Van der Pol oscillators, with $\lambda = 0.3, \omega = \pi$. State variables x_2 plotted against x_1 (left) and x_3 plotted against x_1 (right).

Clearly, just juxtaposing two oscillators is a rather artificial construction. However, if we choose a small positive value for ε, we expect (4.7)-(4.10) again to have a torus as an attractor, close to the torus for $\varepsilon = 0$. Indeed, Figure 4.5 shows phase portraits that are very close to those of uncoupled, juxtaposed oscillators, shown in Figure 4.4. However, when the coupling ε becomes strong, the 4-dimensional system may have asymptotically periodic solutions, as shown in Figure 4.6. This is a form of synchronization between the two oscillators.

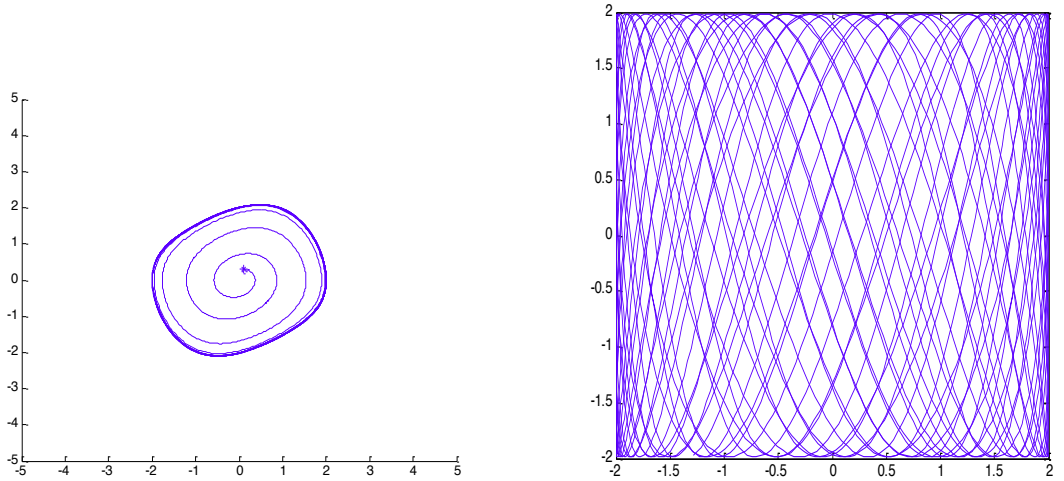

Figure 4.5: Orbits of two weakly coupled Van der Pol oscillators, with $\varepsilon = 0.001, \lambda = 0.3, \omega = \pi$. State variables x_2 plotted against x_1 (left) and x_3 plotted against x_1 (right).

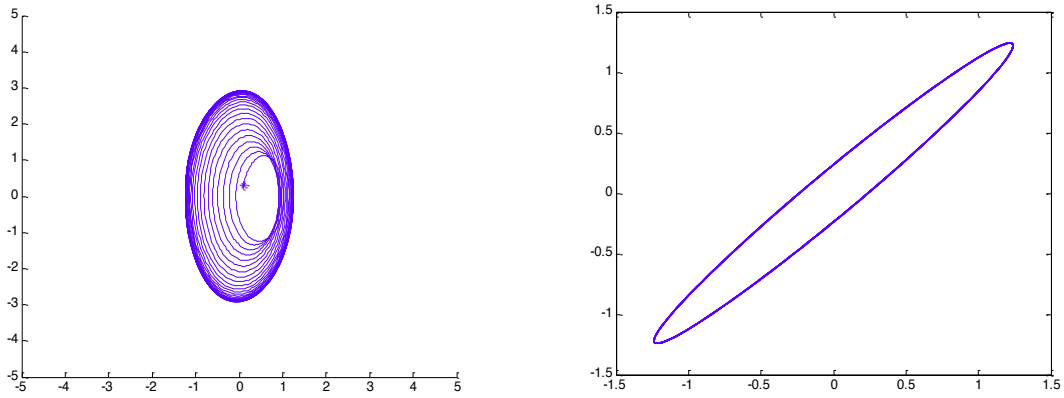

Figure 4.6: Orbits of two strongly coupled Van der Pol oscillators, with $\varepsilon = 10, \lambda = 0.3, \omega = \pi$. State variables x_2 plotted against x_1 (left) and x_3 plotted against x_1 (right).

4.2.4 Example 4: Iterations of the Lozi map

Consider the discrete-time system (4.2) for $n = 2$, with the map F defined by

$$F\begin{pmatrix} x_1 \\ x_2 \end{pmatrix} = \begin{bmatrix} \alpha - 1 - \alpha\,|x_1 + x_2| \\ \beta x_1 \end{bmatrix}, \tag{4.11}$$

which is called the Lozi map. For $\alpha = 1.7$ and $\beta = 0.5$ the system has a chaotic behavior. A solution starting close to its attractor is shown in Figure 4.7. It gives a good idea of the complex geometric structure of the attractor. It is full of layers and holes. Such geometric objects are also called fractals. The salient feature of fractals is that they look the same at all scales. On the left of Figure 4.7, 1000 points of the orbit are represented, which give a good idea of the complex geometric structure of the attractor. On the right 10000 points are plotted. Now the complicated structure is not anymore visible because of the poor resolution of the picture. However, when we enlarge the little rectangle of the right of Figure 4.7, the complicated structure of the attractor becomes again visible (Figure 4.8).

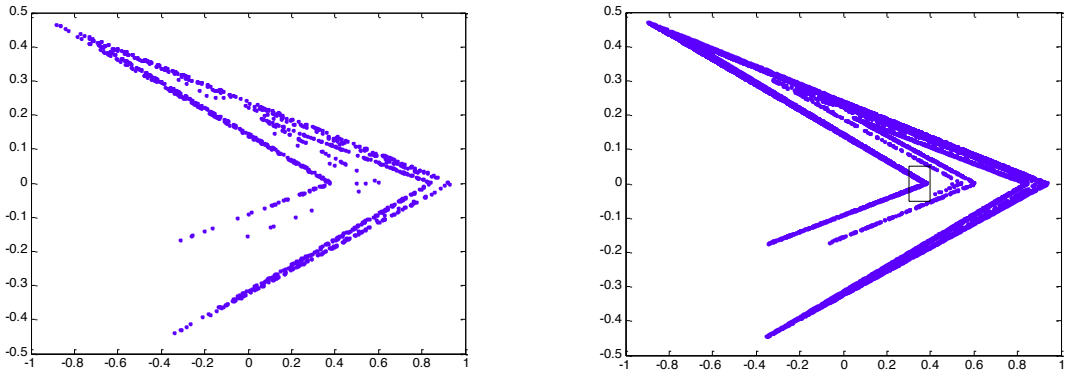

Figure 4.7: Orbits of 1000 iterations (left) and 10000 iterations of the Lozi map, starting close to the attractor of the system.

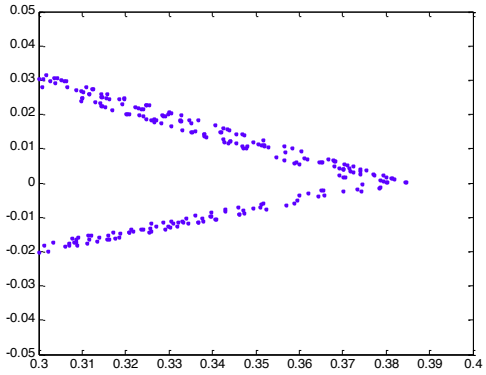

Figure 4.8: Part of the orbit of 10000 iterations of the Lozi map that lies in the small rectangle in the right of Figure 4.7. Note that this enlargement shows again the layered structure of the attractor.

4.2.5 Example 5: Iterated function systems for generating fractals

Instead of studying the fractals as byproducts of dynamical systems, one can try to generate fractals with desired properties by suitably choosing the generating dynamical systems. This is usually done by iterated function systems. These dynamical systems differ from the state equations (4.2) in the sense that they do not describe the trajectories of points in $\mathbb{R}^n$, but the trajectories of sets in $\mathbb{R}^n$.

The construction goes as follows. Let M functions $F_m : \mathbb{R}^n \to \mathbb{R}^n$, $m = 1, \ldots, M$ be given. They are contractions, i.e. they map a bounded volume into a smaller volume. Most often, affine mappings are taken, i.e.

$$F_m(x) = A_m x + b_m$$

where A_m is an $n \times n$ matrix with $\|A_m\| \leq 1$ and b_m is an n-dimensional vector. The functions F_m are applied to sets $\mathcal{S} \subset \mathbb{R}^n$, and we write

$$F_m(\mathcal{S}) = \{F_m(x) \mid x \in \mathcal{S}\}.$$

The trajectory of sets is then constructed by the state equation, where $t \in \mathbb{N}$ denotes the iteration number,

$$\mathcal{S}(t+1) = F_1(\mathcal{S}(t)) \cup \ldots \cup F_m(\mathcal{S}(t)). \tag{4.12}$$

The functions F_m and the initial set $\mathcal{S}(0)$ are usually defined in such a way that they all map $\mathcal{S}(0)$ to a subset of itself and that different sets $F_m(\mathcal{S}(t))$ do not overlap. As an example, take as $\mathcal{S}(0)$ an equilateral triangle and map it by F_1, F_2, F_3 to equilateral triangles of half the original size that are placed to the 3 corners of the original triangle. The union $\mathcal{S}(1)$ calculated according to (4.12) leaves another triangle of half the original size empty. Repeating the iterations (4.12) ad infinitum leads to the fractal called the *Sierpinsky gasket* as the limiting set, as shown in Figure 4.9.

The fractal called the *Barnsley fern* is generated by the four affine functions F_m, $m \in \{1, 2, 3, 4\}$, given by

$$F_m \begin{pmatrix} x_1 \\ x_2 \end{pmatrix} = \begin{bmatrix} r_m \cos\varphi_m & -s_m \sin\psi_m \\ r_m \sin\varphi_m & -s_m \cos\psi_m \end{bmatrix} \begin{bmatrix} x_1 \\ x_2 \end{bmatrix} + \begin{bmatrix} e_m \\ f_m \end{bmatrix}, \tag{4.13}$$

where the parameters are given in Table 4.2.5.

The initial set is an upright rectangle with the origin of the coordinate system at the middle of the lower edge. The surprising resemblance of this and other fractals with objects in nature has lead to the idea to use iterated function systems to code natural images. Note that only a few numbers have

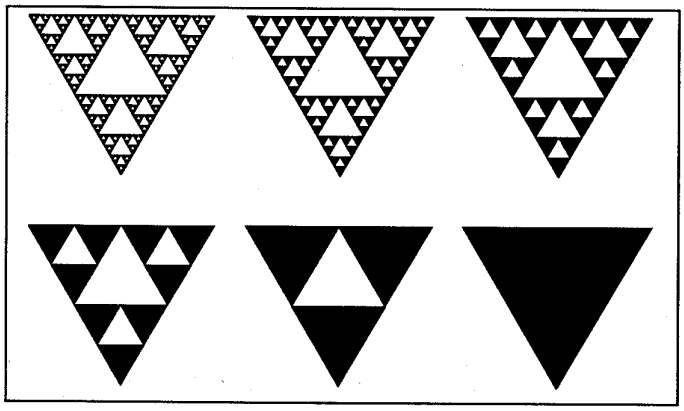

Figure 4.9: Fractal called Sierpinsky gasket and the way it is constructed, from the bottom right to the top left (from H.-O. Peitgen, H.Jürgens, D.Saupe, Fractals for the classroom, Springer-Verlag, New York, 1992).

	Translation		Rotation (in degrees)		Scaling	
m	e_m	f_m	φ_m	ψ_m	r_m	s_m
1	0	1.6	-2.5	-2.5	0.85	0.85
2	0	1.6	-49	49	0.3	0.34
3	0	0.44	120	-50	03	0.37
4	0	0	0	0	0	0.16

Table 4.1: Parameters of the affine functions used to generate the Barnsley fern.

to be known to reconstruct the whole complicated set of Figure 4.10. Depending on the fractalness of regions in an image, this method of image coding can achieve quite high compression rates.

Figure 4.10: Fractal called Barnsley fern (from H.-O. Peitgen, H.Jürgens, D.Saupe, Fractals for the classroom, Springer-Verlag, New York, 1992).